NASA DEVELOP National Program
Massachusetts - Boston

Summer 2024

Narragansett Bay Water Resources

Using Earth Observations to Identify Trends in Harmful Algal Blooms in Narragansett Bay

DEVELOP Technical Report

August 9th, 2024

Mahnoor Naeem (Project Lead)
Isabella Giordano
Samuel Millay
Chloe Rowen

Advisor:
Cédric G. Fichot (Boston University)

Lead:
Madison Arndt (Massachusetts - Boston)

1. Abstract

Narragansett Bay in Rhode Island is known for its quahog, or hard-shell clam, shellfisheries. However, increased levels in harmful algal blooms (HABs) and high phytoplankton biomass events pose threats to quahog populations, creating conditions that limit quahog growth and reproduction. Quahog shortages, along with public health concerns associated with contamination of shellfish from HAB-produced neurotoxins, have contributed to shellfishery closures. NASA DEVELOP partnered with the Environmental Protection Agency's National Health and Environmental Effects Research Laboratory and Rhode Island's Department of Environmental Management to use Earth observations and the partners' in-situ data to visualize phytoplankton bloom events within the bay. We used Sentinel-3 Ocean and Land Color Instrument (OLCI), Landsat 8 and 9 Operational Land Imager (OLI) data to track several proxies of phytoplankton biomass from June 2016 to October 2023. Multiple sensors and in situ datasets were used to assess the feasibility of monitoring phytoplankton biomass accurately in the relatively small sized Narragansett Bay. We determined that Phytoplankton fluorescence line height was the best parameter to monitor phytoplankton biomass in the bay. Although the relatively small size of the bay and the optical complexity of these nearshore waters can pose a challenge, this assessment showed that Earth observations can be a useful complement to the in-situ monitoring of phytoplankton biomass in Narragansett Bay.

Key Terms

Remote sensing, Harmful Algal Blooms, Narragansett Bay, normalized fluorescence line height, chlorophyll-a, Nechad algorithm, Total Suspended Solids, Sentinel-3

2. Introduction

2.1 Background Information

Harmful algal blooms (HABs) are an increasingly pressing environmental concern, characterized by rapid growth of algae that can create hazardous conditions. Increasing global temperatures and influxes of nutrients, such as nitrogen, contribute to the magnitude and frequency of blooms (Dai et al., 2023). In Narragansett Bay, Rhode Island, wastewater treatment centers have been upgraded to control nitrogen loading into the bay and HABs have been closely monitored in-situ due to their potential impacts on the environment, economy, and human safety.

High phytoplankton biomass, upon decomposition, can cause oxygen depletion or anoxic conditions in waterbodies, leading to a decrease in ecosystem productivity, organism growth rates, and respiration rates (Pitcher & Probyn, 2016). Two phytoplankton species of concern identified by our partners were *Pseudo-nitzschia* and the *Margalefidinium polykrikoides. Pseudo-nitzschia* was of concern due to its impact on the economy and public health, as it can produce domoic acid, a neurotoxin, that can contaminate shellfish, leading to shellfishery closures and, if consumed, Amnesiac Shellfish Poisoning (ASP). In severe cases, ASP can lead to memory loss, muscle weakness, and death (Sterling et. al, 2022). Another phytoplankton species, *Margalefidinium polykrikoides,* produces toxins lethal to bivalves, contributing to a decline in quahog populations. The "rust tide," an accumulation of the rust-colored *M. polykrikoides,* negatively impacts tourism (Carney-Almeida et al., 2024).

Narragansett Bay is home to one of the world's longest-running water quality and phytoplankton time series, containing in-situ data samples from as far back as the 1950s. These samples contain information about nutrients, chlorophyll, turbidity, and phytoplankton count. While there are established systems for on-site data in the region, there is a lack of remotely sensed data to track HABs. Although the bay is small, remote sensing can monitor HABs on a larger scale and for extended periods of time. It is difficult for satellite data to detect HABs in thin layers, but it can effectively identify high biomass HABs such as rust tides (Shen et al., 2012). Narragansett Bay lacks previous studies using remote sensing to assess water quality. However, lots of

research has been done on other water bodies and estuaries to monitor HABs using satellite data (Shen et al., 2012; Lopez Barreto et al, 2024).

Chlorophyll fluorescence peak at 683 nanometers is one approach that can facilitate the remote detection of phytoplankton from remote sensing, allowing a visible separation in HABs from other water constituents (Shen et al., 2012; Upadhyay et al. 2023). While other methods of HAB analysis are available with in-situ data, they are not feasible for use on a larger scale. When monitoring the movement of blooms, it is a more viable option to view these large-scale changes using remote sensing capabilities, providing continuous spatial coverage that can be easily accumulated in a time series (Lopez Barreto et al., 2024).

2.2 Study Area & Period

Our study area was Narragansett Bay, which lies within Rhode Island and a small part of Massachusetts. Narragansett Bay is 146 mi² and borders 400 mi of the Rhode Island coastline (Save The Bay, 2023). Providence, the capital and largest city in Rhode Island, borders Narragansett Bay to the north. This was an appropriate study area for the project due to its history of HABs, extensive existing water sample data, and proximity to large human population centers.

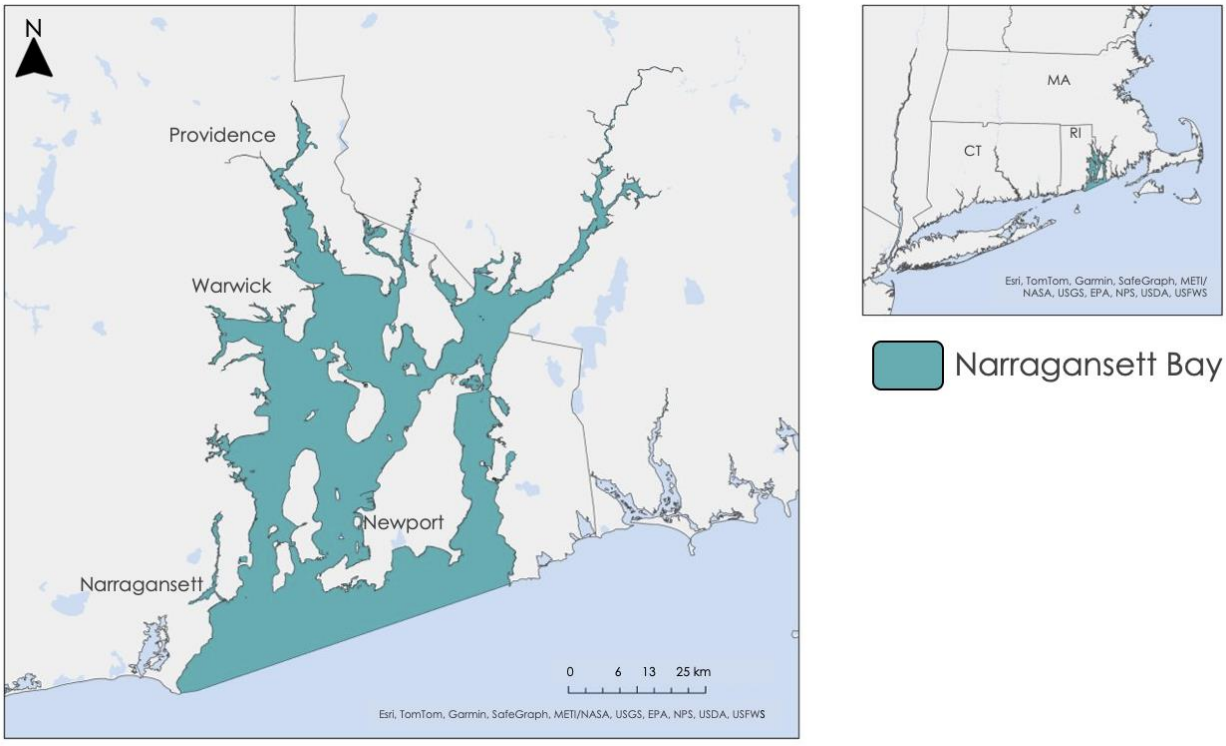

Figure 1. Study area map of Narragansett Bay, RI

Because Senitnel-3A launched in 2016, we gathered satellite data from 2016 to 2023 for this study. Due to elevated levels of HABs in warmer months, we focused our study period on the summer and early fall (June to October each year). This eight-year study period allowed us to focus on the contemporary levels of HABs in Narragansett Bay.

2.3 Project Partners & Objectives

We established partnerships with two experts whose work focuses on monitoring Narragansett Bay. Our partner Autumn Oczkowski is a researcher at the National Health and Environmental Effects Research

Laboratory within the U.S. Environmental Protection Agency (EPA). Her work centers around nutrient dynamics and climate change impacts on coastal areas. We also partnered with David Borkman, Shellfish Water Quality Program Supervisor at the Rhode Island Department of Environmental Management (RIDEM). He specializes in marine phytoplankton and using plankton time series and water quality monitoring for trend prediction. The partners were interested in determining if remote sensing can provide insight on predicting HAB events. We utilized Sentinel-3 Ocean and Land Color Instrument (OLCI) imagery of Narragansett Bay to analyze the presence of HAB occurrences both spatially and temporally. We performed time series analysis using various algorithms to derive the variables for Total Suspended Solids (TSS) and chlorophyll. Monitoring trends in blooms provided valuable insights about what is causing HAB growth and how to carry out future activities in the bay and surrounding areas.

3. Methodology

3.1 Data Acquisition

3.1.1 Sentinel-3 Data Acquisition

We acquired imagery of Narragansett Bay using Sentinel-3 OLCI Earth Observation Full Resolution (EFR) satellite imagery which has a spatial resolution of 300 meters and achieves full Earth coverage daily (EUMETSTAT, 2024). Each OLCI image covers a swath of 1270 kilometers. We downloaded Level 2 imagery of June to October from 2016 to 2023 from NASA's OceanColor Web.

3.1.2 Landsat Data Acquisition

We used Landsat 8 Operational Land Imager (OLI) and Landsat 9 OLI-2 throughout the project. These both cover swaths of 185 kilometers and a given Landsat OLI system cover the Earth every 16 days. They both have resolutions of 30 meters, allowing for spatially detailed imagery of Narragansett Bay, relative to OLCI data. If used together, Landsat 8 and 9 revisit the same area on Earth once every 8 days. We focused on data from June to October throughout our study period, 2016 to 2023. Due to a more recent launch in 2021, Landsat 9 OLI-2 data is limited, as opposed to Landsat 8's launch date in 2013. We acquired Landsat data from Google Earth Engine (GEE). Table 1 shows more information on our data platforms and sensors.

Table 1.
Earth Observations Datasets Used for Data Acquisition

Platform & Sensor	Processing Level	Dates	Acquisition Method	Spatial Resolution	Usage
Sentinel-3 A/B OLCI	Level 2	June – October 2016 - 2023	NASA OceanColor Web	300 meters	nFLH, TSS
Landsat 8 OLI	Level 2	June – October 2016 - 2023	Google Earth Engine	30 meters	NDTI
Landsat 9 OLI-2	Level 2	June – October 2022 - 2023	Google Earth Engine	30 meters	NDTI

3.1.3 In-situ Data Acquisition

To verify our remotely sensed data, we analyzed data from our partners at the EPA and RIDEM. The EPA dataset took water quality samples, including chlorophyll-a and TSS measurements, from multiparameter water quality sensors called YSI sondes located at 8 different sampling stations throughout the Bay. YSI stands for Yellow Springs Instruments which is a part of Xylem Analytics. (YSI, n.d.) The company is a leading provider in water measurement solutions. The RIDEM dataset shows chlorophyll-a measurements taken every 15 minutes. YSI sondes collected the data at 15 active sites in the bay from 11 buoy sites and 4 fixed dock sites. We received this data directly from our partners and used Microsoft Excel to clean the data and graph the chlorophyll (in micrograms/liter) and TSS (in milligrams/liter) from within our study period.

These graphs provided us with information on peak events and seasonal trends for the mentioned observed environmental variables.

3.2 Data Processing

3.2.1 Sentinel-3 Data Processing

We utilized the Remote sensing reflectance (Rrs) bands pf Sentinel-3 OLCI Ocean Color (OC) to calculate the Normalized Fluorescence Line Height (nFLH) product and TSS values. We processed and visualized the images using SeaDAS 8.2.0, a NASA-generated software specializing in displaying ocean color data. We used Fluorescence Line Height (FLH) to detect chlorophyll and compared it to field measurements. FLH is commonly used in small scale HAB sensing because it is less sensitive to interference by Colored Dissolved Organic Matter (CDOM). CDOM absorbs the same wavelengths as chlorophyll in the blue-green spectra, which could skew results if a blue-green reflectance band ratio is used as proxy for phytoplankton biomass. In contrast, FLH uses the red portion of the electromagnetic spectrum to sense chlorophyll, thereby limiting CDOM interference (Shen et. Al, 2012). We calculated the FLH using Eq. (1) where Rrs_F is the remote sensing reflectance at the fluorescence peak band λ_F, and Rrs_R and Rrs_L are the remote sensing reflectance at the shorter and longer baseline bands, λ_R and λ_L. Fluorescence bands are measured in nanometers and FLH is measured in per steradian (sr^{-1}). To detect *M. polykrikoides,* we used wavelengths 660 nm, 680 nm, and 745 nm for λ_F, λ_R, and λ_L (Zhao et. al., 2022). We visualized these images using SeaDAS and used the deep color palette with a range of 0 to 0.1.

We also used equation 2 from Table 2, which is referred to as the Nechad Algorithm, to calculate a TSS estimate from remote sensing data using MATLAB R2022b. The equation models TSS concentration, *S,* where ρ_w described water reflectance and A^ρ, B^ρ, and C^ρ were calibration coefficients calculated by specific wavelengths (Nechad et al., 2010; Morel & Gentili, 1991). The units for *S* are FNU (Formazin Nephelometric Unit). For our analysis, we used bands of 665 nm and 709 nm.

Another proxy we tested against the in-situ chlorophyll-a data was the ratio between OLCI bands 709 nm and 665 nm. The reason these two bands were chosen is because chlorophyll-a has high absorption in the red region of the electromagnetic spectrum which is around 665 nm which means that reflectance is low at this wavelength. The 709 nm band is used because that is where there is a peak in reflectance caused in part by particle scattering. The ratio of these bands is a potential proxy for chlorophyll concentrations. We implemented this using Equation 4 in Table 2.

3.2.2 Landsat Data Processing

As the project used Collection 2 Level 2 Landsat Data, there was no need for further atmospheric correction. Using Landsat 8 OLI and Landsat 9 OLI-2 in Google Earth Engine, we calculated the Normalized Difference Turbidity Index (NDTI), shown in Equation 3 on Table 2. More negative values indicated less turbid waters and values closer to zero indicated more turbid waters or sun glint (Bid & Siddique, 2019). NDTI used the red and green bands as a proxy for water turbidity, comparing the two in terms of their electromagnetic reflectance. The clearer the water, the higher the electromagnetic reflectance, and conversely, the more turbid the water, the lower the electromagnetic reflectance (Lizcano-Sandoval et al., 2022). Additionally, as we utilized Level 2 Collection 2, there was no need to use further atmospheric correction techniques.

Table 2.

Equations used in pre-processing of Earth Observations

Equation Number	Equation Title	Equation
1	nFLH	$FLH = Rrs_F - \left[Rrs_R + \frac{\lambda_R - \lambda_F}{\lambda_R - \lambda_L}(Rrs_L - Rrs_R)\right]$

2	Nechad algorithm	$S = \frac{(A^{\rho}\rho_{\omega})}{\left(\frac{1-\rho_{\omega}}{C^{\rho}}\right)} + B^{\rho}$
3	NDTI	$NDTI = \frac{red\ band - green\ band}{red\ band + green\ band}$
4	Ratio	$\frac{R_{rs}(709)}{R_{rs}(665)}$

3.2.3 In-situ Data Processing

We used Microsoft Excel to process the in-situ data from RIDEM and the EPA. The RIDEM data from the YSI sondes retrieved data every 15 minutes. To directly compare the sondes data to the satellite data, we isolated the timings from around the time that Sentinel-3 OLCI takes images of Narragansett Bay which is from 10 a.m. to 2 p.m. We then took the mean chlorophyll-a for each day at a given station. We focused our analysis on the stations in the western bay. The RIDEM stations we analyzed include B2 (North of Prudence Island), B3 (Conimicut Point), B6 (Mountain View), and B7 (Quonset Point) (Figure G1).

For the EPA data, we looked at stations 1 through 5, which all lie in the Western Passage. TSS measurements were taken from the EPA data to compare to our remote sensing TSS algorithms. Since the EPA only collects in-situ data a few times a month, we had very few data points for TSS. To directly compare the TSS datasets, we only used points that were taken on the same day for both in-situ and satellite data. We took the mean values of each day for both datasets to compare and analyze the values.

3.3 Data Analysis

Collaborators from the EPA and RIDEM provided us with extensive in-situ data, including measurements of chlorophyll, turbidity, and cell count from multiple sondes and sample locations throughout the bay (NBFSMN (2016-2023), Pimenta et al. (2023). We graphed chlorophyll and TSS data for each year in Microsoft Excel to identify peak events and trends in the timing of phytoplankton blooms. Based on these graphs, we established a seasonal study period of June-October for each year.

The MATLAB script updated the NetCDF files for each satellite image of the bay. We then used these files to analyze the parameters (chlorophyll and TSS) within the bay. To determine which parameter we would use as a proxy for phytoplankton, we identified 3x3 pixel areas (900x900m) around 7 EPA sondes and 7 RIDEM sondes from the Upper Bay to the Lower Bay used for on-site data measurements. Using these points, we directly compared the data taken from water sampling to the Sentinel-3 data processed in MATLAB. From this, we compared nFLH and the OLCI-generated chlorophyll-a values to the onsite measurements of chlorophyll-a, and the Nechad TSS & NDTI products to TSS concentration to determine which remote sensing proxy best matches the in-situ measurements. We created a time series on Excel comparing the parameters to the sample data to see which had the strongest correlation. We also graphed the in-situ and remotely sensed data sets against each other and generated the R^2 values. After determining that FLH and the Nechad algorithm were the closest proxies to chlorophyll-a and TSS, and, in turn, phytoplankton, we focused our study on it. We derived nFLH and Nechad in the bay from R 4.4.1, and then plotted them in Microsoft Excel. We plotted nFLH and Nechad TSS time series to show phytoplankton biomass fluctuations over our study period and visualized our results using SeaDAS software (Figures E1 & F2).

4. Results & Discussion

4.1 Analysis of Results

Overall, we found that nFLH was the best proxy to track chlorophyll in Narragansett Bay and the Nechad algorithm was the best to track TSS. We used the extensive in situ dataset to compare the results of the algorithms run on the satellite images. After testing the RIDEM chlorophyll-a data with nFLH and the ratio between bands 709 and 665, we determined the chlorophyll-a and nFLH have a stronger correlation. The ratio between Sentinel-3 OLCI band 709 and band 665 did not yield a high correlation between the in-situ

chlorophyll-a values. A possible reason for the low correlation is because of its higher vulnerability to interference from substances like CDOM and non-algal particles in the water. We used YSI sondes to calculate in-situ data which used fluorescence to measure chlorophyll-a since it was a more direct comparison to the nFLH calculation (YSI, n.d.). For this reason, it is understandable that the nFLH performed better when compared to the in-situ data. To directly compare the datasets, we isolated the points for days where both in situ and satellite data was present. As seen in the charts in Figures 2, A1 and A2, at stations B3 and B6 in the West Passage, nFLH correlates much more with in-situ chlorophyll-a than the Ratio between bands 709 and 665 seen in Figure 3.

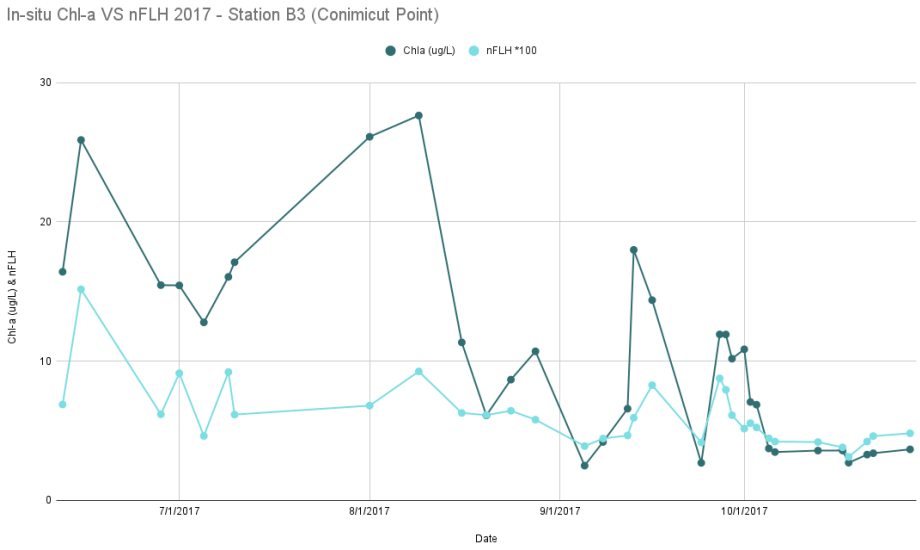

Figure 2. Time series visualization of in-situ chl-a values vs. nFLH (sr-1) values for the year 2017

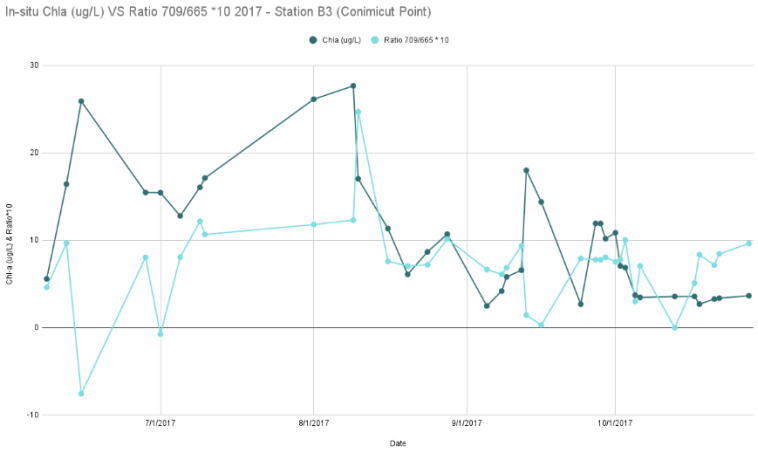

Figure 3. Time series visualization of in-situ chl-a values vs. Sentinel-3 OLCI band ratio values of bands 709 and 665 for the year 2017

Though we found that nFLH is the best proxy for tracking chlorophyll-a in the bay based on its performance against the in-situ data, nFLH was not able to pick up on some big bloom events such as the ones seen in 2018 and 2020 in Figures A1 and A2. It is unclear why the proxy does not pick up high values when the in-situ chlorophyll-a is excessively high and needs a more in-depth study. From these results we see that Sentinel-3 is effective in displaying trends when chl-a values remain relatively normal, and it does not perform well during excessive biomass events.

We also compared the in-situ chlorophyll-a data with the built in Sentinel-3 OLCI chlorophyll-a (chl-a) data, which have units of ug/L and mg/m^3 respectively. As these units are 1:1, the OLCI chl-a values should have been comparable and highly correlated with the in-situ chl-a. However, we found the OLCI chl-a values were much higher and not correlated. One of the main reasons for this discrepancy was that Narragansett Bay is very small, and the water body is relatively dark. Sentinel-3 calculated chl-a using the blue and green part of the electromagnetic spectrum. (EUMETSAT, 2021). It is not recommended to use the Sentinel-3 values for coastal water bodies, which was also seen in our results. The graphs in Figures 4, B1, and B2 show the correlation between in-situ chl-a and OLCI chl-a from station B6, in the middle of the bay.

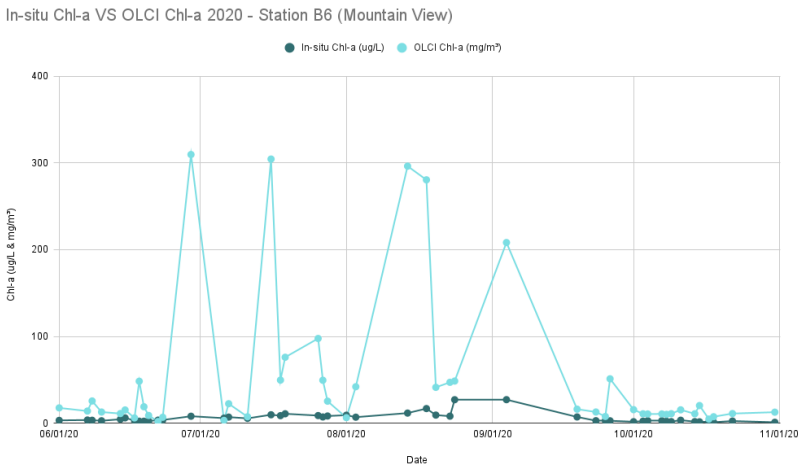

Figure 4. Time series visualization of in-situ chl-a values vs. Sentinel-1 chl-a values for the year 2020

The OLCI chl-a values differed greatly from the in-situ dataset. As a result of this poor correlation, we deduced that nFLH is a better proxy for tracking chlorophyll-a in Narragansett Bay than the built in Sentinel-3 OLCI chl-a calculation.

After fitting a linear trend between the in-situ chlorophyll-a and each of the remote sensing chlorophyll-a proxies, we determined that nFLH had the highest correlation, as shown in Figures 5-7.

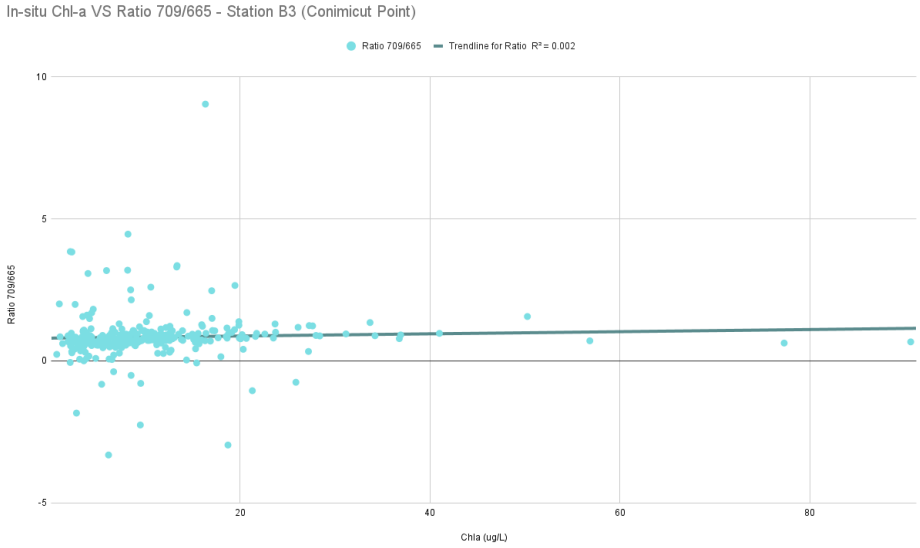

Figure 5. Low correlation (R^2 of 0.002) between in-situ chl-a and the Sentinel-3 OLCI band ratio values

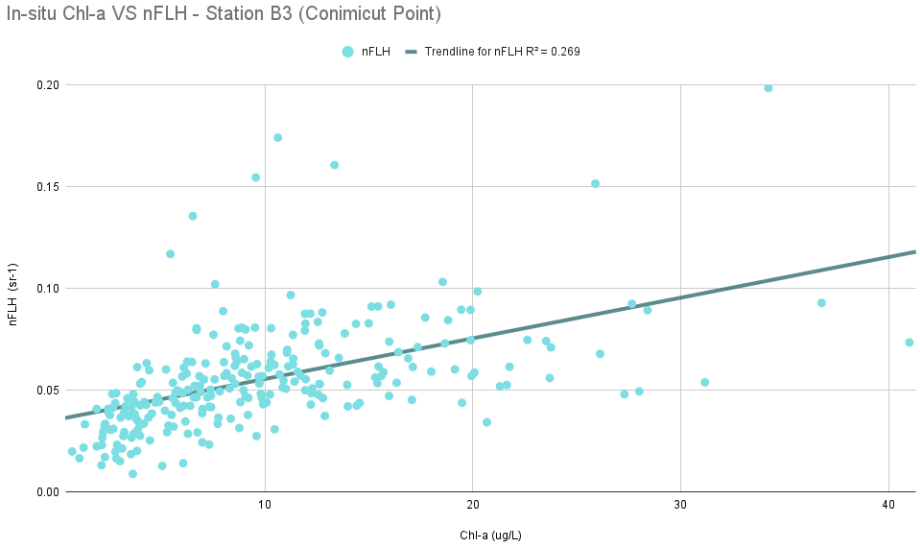

Figure 6. Modest correlation (R^2 of 0.269) between in-situ chl-a and nFLH (sr-1) values

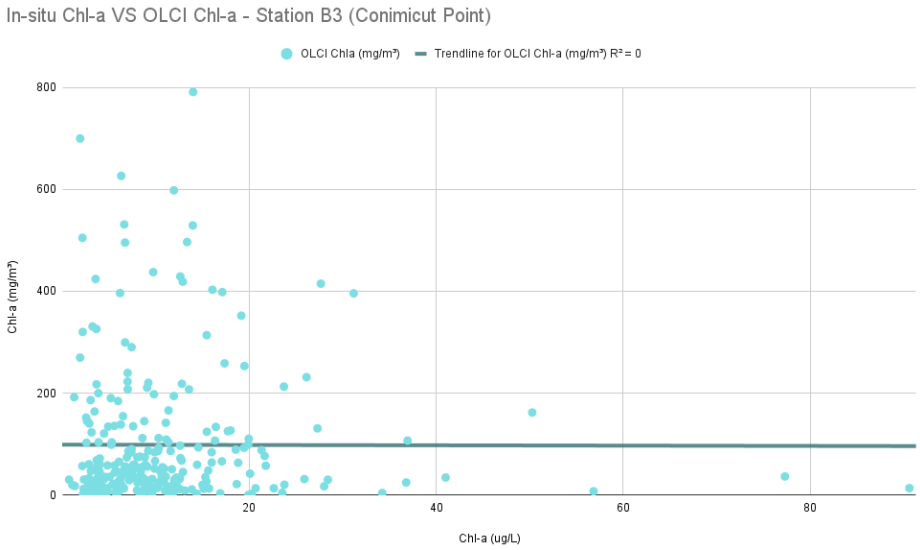

Figure 7. No correlation between in-situ chl-a and OLCI chl-a values

Since there was not a substantial amount of in-situ data for TSS and turbidity, a robust analysis was not possible. However, we graphed the Nechad TSS values against TSS field values collected on the same day around the same location in Narragansett Bay to better analyze the correlation. We also inserted the R^2 value of the graph's linear relationship, which was 0.323. For NDTI, we created a time series for each year showing the mean NDTI values.

The graphs showed stronger correlation between TSS field data and Nechad products than NDTI. In addition, Landsat-8 and 9 had limited data, resulting in as few as 3 data points per year. The NDTI graphs showed seemingly random dips and peaks in turbidity values that did not align with the observed seasonal peaks in July and August (Figure C1). We concluded that the Nechad algorithm was more accurate at remotely sensing TSS than NDTI.

We visualized both variables in SeaDAS to further investigate the overall concentration of chl-a and TSS throughout the bay and where and when high biomass events occurred. We selected the year 2016 due to the varied concentrations of these 2 variables in the bay throughout the months, allowing for easy interpretation of peaks and dips in values. As seen in Figure 8, E1, and F1, FLH levels peaked in the months of July and August and began to lessen in Week 4 of August. Chl-a concentrations were highest in the upper bay and lower in the lower bay, which is closer to the open ocean. In the 2016 Nechad TSS visualization in Figure D1, the peak values occurred in weeks 1, 3, and 4 of July and week 3 in August. TSS was relatively higher near the edges of the bay and even though the focus of the study is on the West passage, the visualizations show higher TSS in Sakonnet which is the eastern part of the bay (Figures D1, E2, and F2).

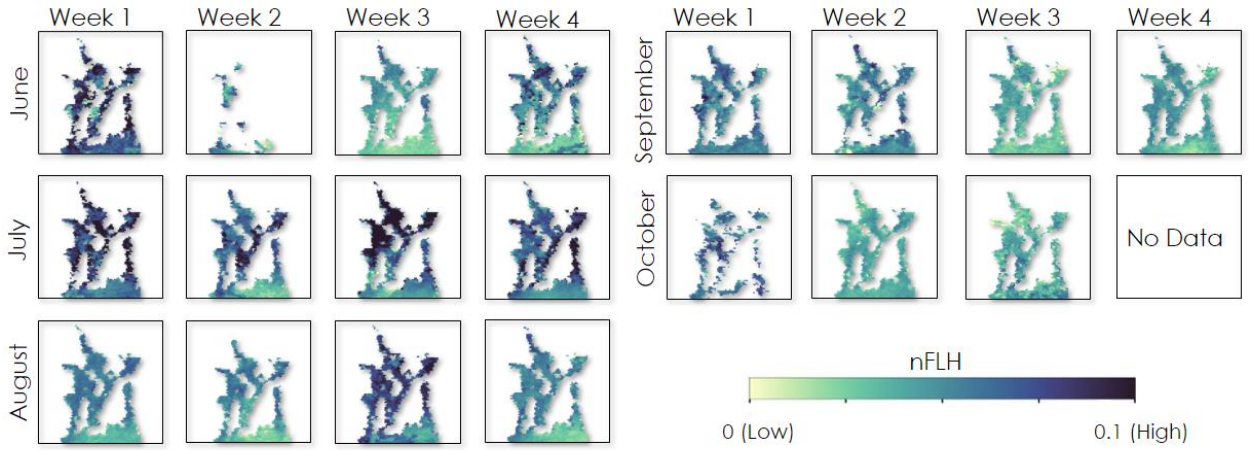

Figure 8. SeaDAS visualization of nFLH (sr-1) through the months of June-October in 2016. Note that while an nFLH minimum for water quality metrics varies by location, a detectable fluorescence signal classifies an individual pixel of having a bloom (Dai et al., 2023).

4.2 Errors & Uncertainties

Errors throughout this project arose mainly due to our data acquisition methods' restrictions. The Sentinel-3 OLCI sensor has a spatial resolution of 300 meters. While we were still able to gather large amounts of data, this reduced the level of detail in which we could study the bay due to its small size. Cloud coverage also restricted many of our satellite images. Often, clouds obstructed the satellite's view of the bay and made for incomplete imagery.

This cloud coverage was also a hinderance for our Landsat-8 OLI and Landsat-9 OLI 2 data; however, the general lack of data across the time series was the primary issue with these two satellites. They produced very few images every summer, resulting in small amounts of data that we could hardly use, given the low revisit and the cloud frequencies. This is partially why we chose Sentinel-3 OLCI to be our primary remote sending method, with Landsat-8 OLI and Landsat-9 OLI 2 as supplements. Additionally, it is important to note that while we elected not to incorporate Sentinel-2 into the project, it's high spatiotemporal resolution may prove beneficial in related future projects.

There were also some limitations to the in-situ data. The RIDEM dataset did not provide turbidity measurements, restricting our comparisons to just the chlorophyll-a values and TSS. The EPA gathered data much less frequently than we needed, with measurements only every week. This dataset sometimes had even larger gaps, for example, in the Summer of 2020, likely due to the pandemic. The in-situ data was also limited to the locations of their sensors in the bay. Even though the EPA and RIDEM have extensive data acquisition programs in Narragansett Bay, we could only compare our data to the exact location of their sondes and sensors. This did not prove to be a very large inconvenience due to many of their sensors being in the West Passage of the bay where we focused much of our research. In addition, we only compared satellite data and onsite data taken on the same day and around the same time of day to ensure accuracy. This did not limit our chlorophyll-a comparisons as much as it did our TSS comparisons, as TSS concentrations at the EPA were taken only a few times a month.

Upon comparison with in-situ data, we noticed that there were patterns as to where our remote sensing data was not accurate. The largest differences between satellite and on-site results occurred during large bloom events (such as August 2018 or July 2020; Figures A1 & A2). When the in-situ chl-a was excessively high, the nFLH did not pick up comparably high values. This pointed to Sentinel-3 not being well-suited to measuring peak events in the bay and being far more accurate during periods of lower biomass.

4.3 Feasibility & Partner Implementation

Our findings suggested that Earth observations can possibly serve as a tool to facilitate the monitoring phytoplankton biomass in Narragansett Bay for future phytoplankton bloom analysis. Through our study, we found that utilizing Sentinel-3 OLCI to track both chlorophyll-a and TSS levels proved useful in that remotely sensed values aligned with the in-situ values provided by our partners. To carry out future analysis, we suggest using nFLH values to best estimate phytoplankton biomass levels and the Nechad algorithm to measure TSS. Our process could be replicated by making use of these methods and utilizing the transect coordinates to maintain consistency in measuring the West Passage of Narragansett Bay. These transect points can be seen in Figure G1.

The previously described Earth observations and methods can be effective tools for monitoring small bodies of water like Narragansett Bay. Methods of HAB analysis that did not function well included the use of Sentinel-3's built-in chl-a sensor to measure chlorophyll-a levels. We attributed the inaccuracy to the use of the blue-green spectra in the OLCI chl-a's sensing of chlorophyll-a, which can be prone to sun glint or other discrepancies in waterbodies like Narragansett Bay. To accurately measure chlorophyll-a levels, the use of nFLH was necessary to obtain accurate and similar results to the in-situ values. NDTI did not serve as a useful proxy in measuring turbidity due to the bay's small area and lack of image availability from Landsat 8 and 9.

5. Conclusions

In summary, we found that it is feasible to use satellite remote sensing of Narragansett Bay in tandem with in-situ data to view and assess certain water quality indicators. Because it had the relatively highest correlation to the abundant chl-a in-situ data, we recommend using nFLH as a direct proxy to biomass within the bay. This was overall the strongest comparison, with only marginal differences, especially during large bloom events. While there was also a strong correlation between satellite and in-situ TSS, we caution partners in the use of this, as we had far fewer datapoints in our comparison due to a lack of in-situ measurements. We advise using the Nechad algorithm outlined in 3.2.2 during data processing for TSS.

Through remote sensing techniques in this project, we identified trends in biomass events in Narragansett Bay. We noticed large increases in nFLH consistently in July and August during our study period, with these events happening throughout the bay. The ability to visualize biomass events is crucial in the maintenance and health of any body of water.

Based on the promising conclusions from our data analysis, our Rhode Island partners now have more ability to implement remote sensing methods in their work. While they have had access to a robust in-situ time series for many years, through our analysis we have found that synoptic satellite remote sensing data can be a strong complement to the existing data. Currently, our partners' on-site data is more reliable than remote sensing, given the scope and resources of their ongoing study of the bay; however, remote sensing can build off this strong foundation to further our partners' understanding of the bay. For example, visualizations of both nFLH and the Nechad TSS product throughout time can help depict patterns in algae movement, aiding in tracking and predicting biomass events. These parameters are the most effective proxies for phytoplankton blooms in a relatively small water body such as Narragansett Bay. As remote sensing technology continuously improves, this satellite data will become more reliable in providing stand-alone products for use in Narragansett Bay.

6. Acknowledgements

The Team:

- Mahnoor Naeem (Project Lead)
- Isabella Giordano
- Samuel Millay
- Chloe Rowen

Center Lead:

- Madison Arndt

Science Advisor:

- Cédric Fichot

Partners:

- Autumn Oczkowski
- David Borkman

This material contains modified Copernicus Sentinel data (2016-2023), processed by ESA.

Any opinions, findings, and conclusions or recommendations expressed in this material are those of the author(s) and do not necessarily reflect the views of the National Aeronautics and Space Administration.

This material is based upon work supported by NASA through contract 80LARC23FA024.

7. Glossary

ASP – Amnesiac Shellfish Poisoning
Chl-a – Chlorophyll-A
Earth Observations – Satellites and sensors that collect information about the Earth's physical, chemical, and biological systems over space and time
FLH – Fluorescence Line Height
HAB – Harmful Algal Bloom
MSI – Multi Spectral Instrument
nFLH - Normalized Fluorescence Line Height
NDTI – Normalized Difference Turbidity Index
OLCI – Ocean and Land Color Instrument
OLI – Operational Land Imager
Quahog – a hard-shell clam native to the East Coast of the USA
RIDEM – Rhode Island Department of Environmental Management
Rrs – Remote Sensing Reflectance
TSS –Total Suspended Solids
YSI sondes – Multiparameter water quality sensors produced by Yellow Springs Instruments.

8. References

Bid, S. & Siddique, G. (2019). Identification of seasonal variation of water turbidity using NDTI method in Panchet Hill Dam, India. *Modeling Earth Systems and Environmen*t, 5. https://doi.org/10.1007/s40808-019-00609-8

Carney-Almeida, J., Sonnet, V., Mouw, C. B., Rines, J., Ciochetto, A. B., & Puggioni, G. (2024). Detecting Margalefidinium polykrikoides through high-frequency imagery: Example of a bloom formation, environmental conditions, and phytoplankton community composition changes. *Harmful Algae,* 136, 102619. https://doi.org/10.1016/j.hal.2024.102619

Dai, Y., Yang, S., Zhao, D, Hu, C., Xu, W., Anderson, D.A., Li, Y., Song, X.P., Boyce, D.G., Gibson, L., Zheng, C., & Feng, L. (2023). Coastal phytoplankton blooms expand and intensify in the 21st century. *Nature* 615, 280–284. https://doi.org/10.1038/s41586-023-05760-y

EUMETSAT. (2024) *Sentinel-3 OLCI Level 1 Data Guide.* https://user.eumetsat.int/resources/user-guides/sentinel-3-olci-level-1-data-guide#ID-Product-quality

EUMETSAT. (2021) *Sentinel-3 Product Notice - OLCI Level 2 Ocean Colour, Collection 3*. https://www.eumetsat.int/ocean-colour-services?lang=EN

Landsat Collection 2 Surface Reflectance | U.S. Geological Survey. (2024). Retrieved August 6, 2024, from https://www.usgs.gov/landsat-missions/landsat-collection-2-surface-reflectance

Lopez Barreto, B. N., Hestir, E. L., Lee, C. M., & Beutel, M. W. (2024). Satellite Remote Sensing: A Tool to Support Harmful Algal Bloom Monitoring and Recreational Health Advisories in a California Reservoir. *Geohealth, 8*(2). https://www.ncbi.nlm.nih.gov/pmc/articles/PMC10885757/

Lizcano-Sandoval, L., Anastasiou, C., Montes, E., Raulerson. G., Sherwood, E., & Muller-Karger, F.E. (2022). Seagrass distribution, areal cover, and changes (1990–2021) in coastal waters off West-Central Florida, USA. *Estuarine, Coastal and Shelf Science* 279, 0272-7714. https://doi.org/10.1016/j.ecss.2022.108134

Morel, A. & Gentili, B. (1991). Diffuse reflectance of oceanic waters: its dependence on Sun angle as influenced by the molecular scattering contribution. *Applied Optics*, *30*, 4427-4438. https://doi.org/10.1364/AO.30.004427

Narragansett Bay Fixed-Site Monitoring Network (NBFSMN). (2016-2023). *Datasets*. Rhode Island Department of Environmental Management, Office of Water Resources. https://dem.ri.gov/environmental-protection-bureau/water-resources/research-monitoring/narraganset-bay-assessment-0

NASA Ocean Biology Processing Group. (2020a). *Sentinel-3A OLCI Earth-observation, Full Resolution (EFR) Ocean Color (OC) Data* [dataset]. NASA Ocean Biology Distributed Active Archive Center. https://doi.org/10.5067/SENTINEL-3A/OLCI/L2/EFR/OC/2022

NASA Ocean Biology Processing Group. (2020b). *Sentinel-3B OLCI Earth-observation, Full Resolution (EFR) Ocean Color (OC) Data* [dataset]. NASA Ocean Biology Distributed Active Archive Center. https://doi.org/10.5067/SENTINEL-3B/OLCI/L2/EFR/OC/2022

Nechad, B., Ruddick, K. G., & Park, Y. (2010). Calibration and validation of a generic multisensor algorithm for mapping of total suspended matter in turbid waters. *Remote Sensing of Environment, 114*(4), 854-866. https://doi.org/10.1016/j.rse.2009.11.022

Pimenta, A. R., Hanson, A., Cobb, D., Schwartz, M., Coiro, L., Mckinney, R., Johnson, R., Balint, S., & Oczkowski, A. (2023). Water Quality Data for Narragansett Bay, RI (USA) from 2014 to 2022 [Data set]. Zenodo. https://doi.org/10.5281/zenodo.10403215

Pitcher, G. C. & Probyn, T. A. (2016). Suffocating phytoplankton, suffocating waters—Red tides and anoxia. *Frontiers in Marine Science*, *3*. https://doi.org/10.3389/fmars.2016.00186

Save the Bay. (2023). Facts & Figures. Save the Bay, Inc. https://savebay.org/bay_issues/facts-figures/

Shen, L., Xu, H., & Guo, X. (2012). Satellite remote sensing of harmful algal blooms (HABs) and a potential synthesized framework. *Sensors*, *12*(6), 7778–7803. https://doi.org/10.3390/s120607778

Sterling, A.R., Kirk, R.D., Bertin, M.J., Rynearson, T.A., Borkman, D.G., Caponi, M.C., Carney, J., Hubbard, K.A., King, M.A., Maranda, L., McDermith, E.J., Santos, N.R., Strock, J.P., Tully, E.M., Vaverka, S.B., Wilson, P.D., & Jenkins, B.D. (2022), Emerging harmful algal blooms caused by distinct seasonal assemblages of a toxic diatom. *Limnology and Oceanography, 67*(11), 2341-2359. https://doi.org/10.1002/lno.12189

Upadhyay Staehr, S., Holbach, A. M., Markager, S., & Upadhyay Staehr, P. A. (2023). Exploratory study of the Sentinel-3 level 2 product for monitoring chlorophyll-a and assessing ecological status in Danish seas. *Science of The Total Environment, 897*, 165310. https://doi.org/10.1016/j.scitotenv.2023.165310

YSI. (n.d.). *6025 chlorophyll sensor*. https://www.ysi.com/accessory/id-6025/6025-chlorophyll-sensor

Zhao, M., Bai, Y., Li, H., He, X., Gong, F., & Li, T. (2022). Fluorescence line height extraction algorithm for the Geostationary Ocean Color Imager. *Remote Sensing, 14*(11), 2511. https://doi.org/10.3390/rs14112511

9. Appendices

Appendix A: *In situ Chl-a VS nFLH Timeseries at Station B6 (Mountain View)*

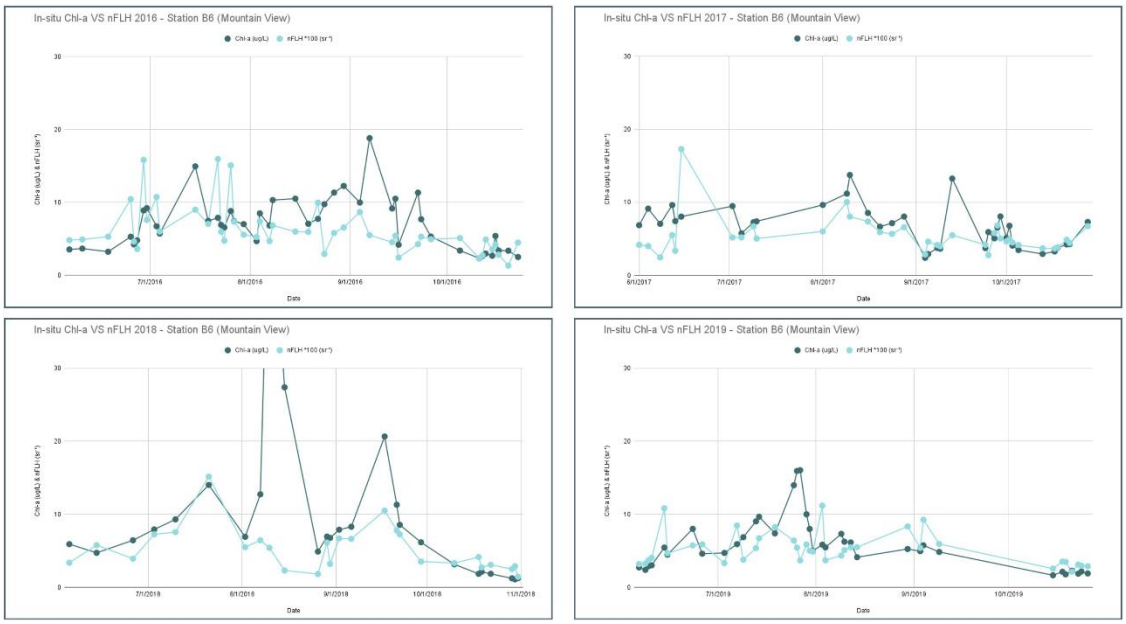

Figure A1. In-situ Chl-a (ug/L) VS nFLH (sr-1) at Station B6 for years 2016 to 2019

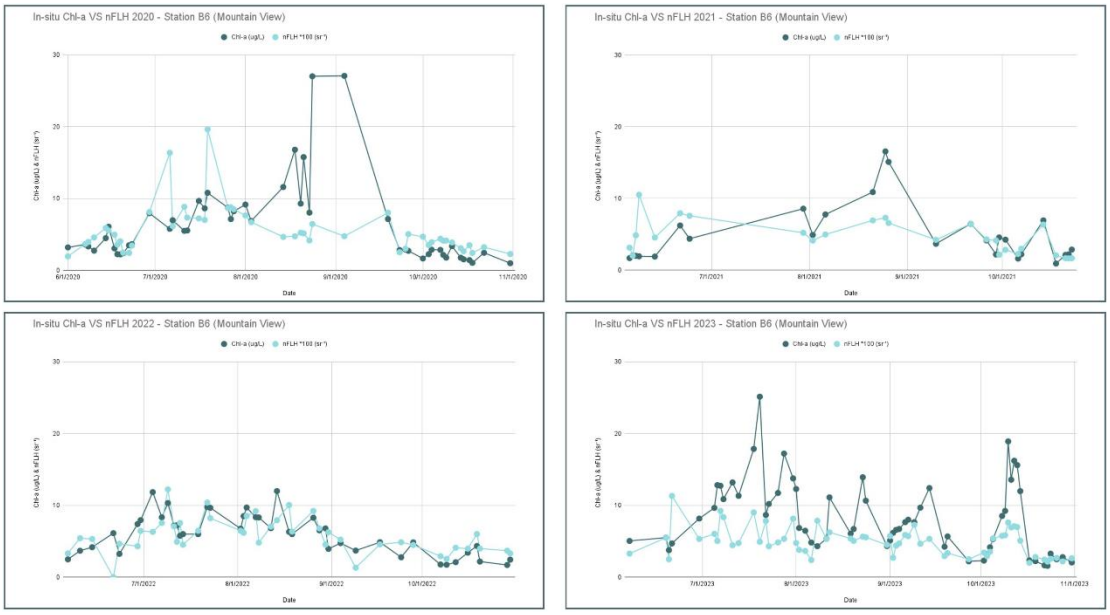

Figure A2. In-situ Chl-a (ug/L) VS nFLH (sr-1) at Station B6 for years 2020 to 2023

Appendix B: *In situ Chl-a VS OLCI Chl-a Timeseries at Station B6 (Mountain View)*

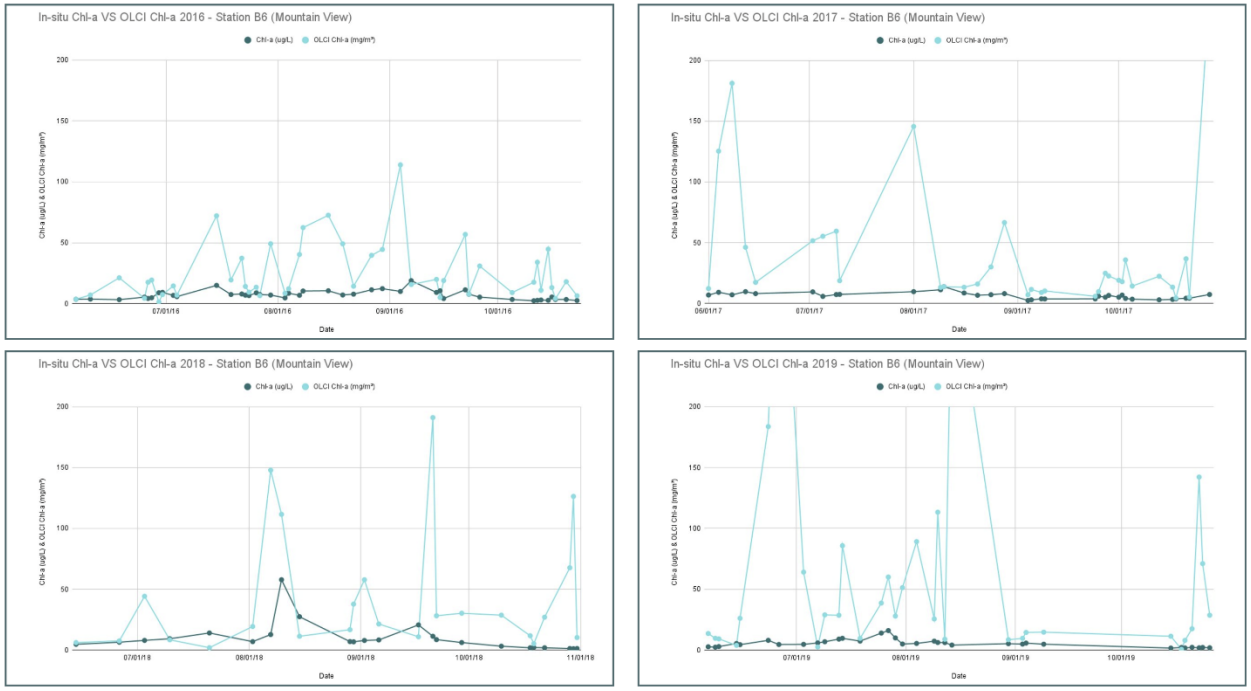

Figure B1. In-situ Chl-a (ug/L) VS OLCI Chl-a (mg/m^3) at Station B6 for years 2016 to 2019

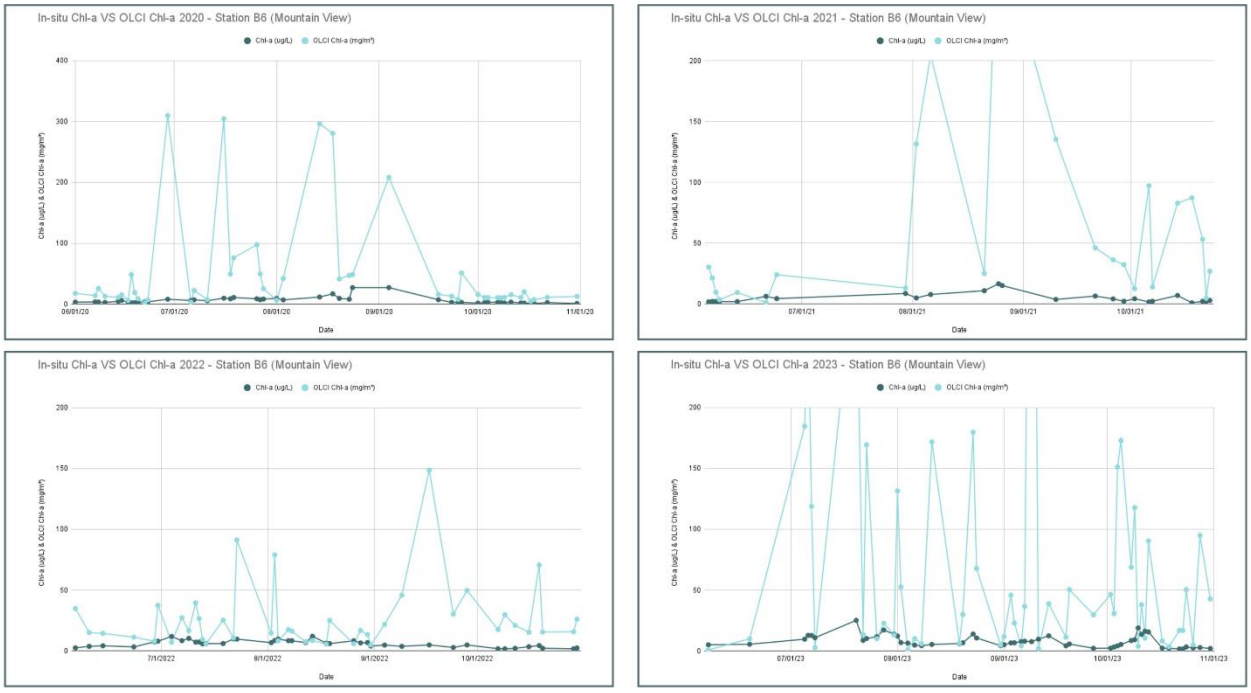

Figure B2. In-situ Chl-a (ug/L) VS OLCI Chl-a (mg/m^3) at Station B6 for years 2020 to 2023

Appendix C: *Normalized Difference Turbidity Index Timeseries calculated using Landsat 8 & 9*

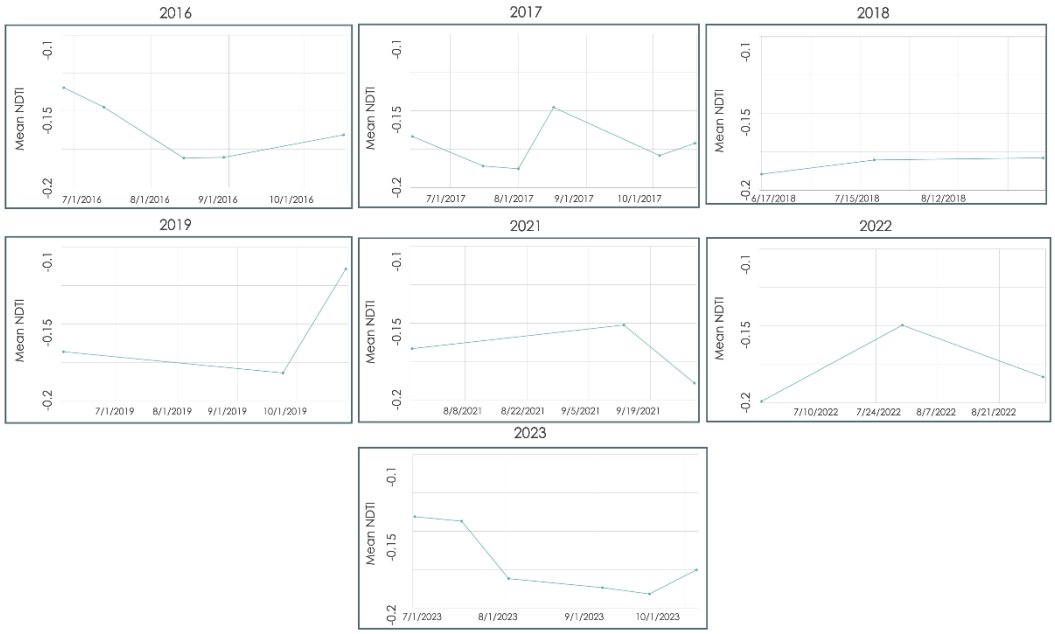

Figure C1. NDTI Timeseries for years 2016, 2017, 2018, 2019, 2021, 2022, 2023

Appendix D: *Weekly Composites for TSS in the year 2016*

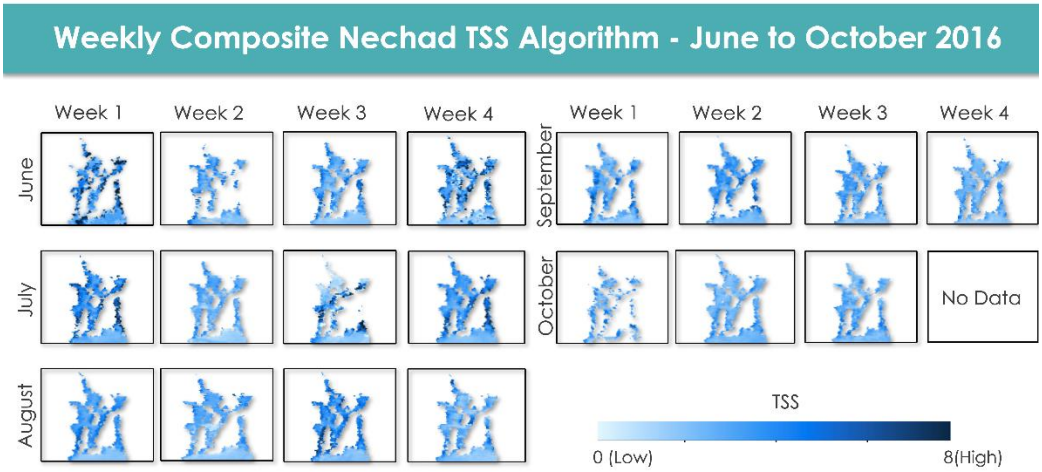

Figure D1. Weekly TSS values for 2016 visualized in SeaDAS with light blue representing low values and dark blue indicating high values.

Appendix E: *Weekly Composites for nFLH and TSS in the year 2018*

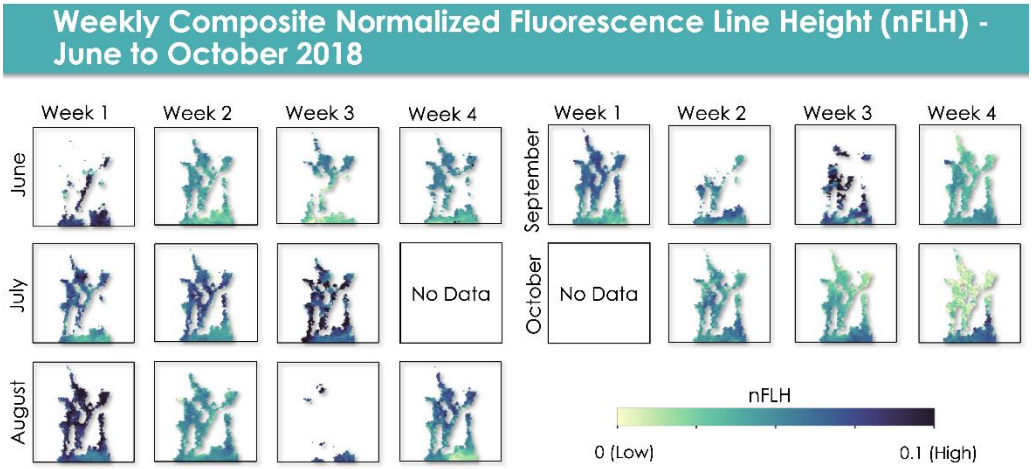

Figure E1. Weekly nFLH values for 2018 visualized in SeaDAS with yellow representing low values and dark blue indicating high values.

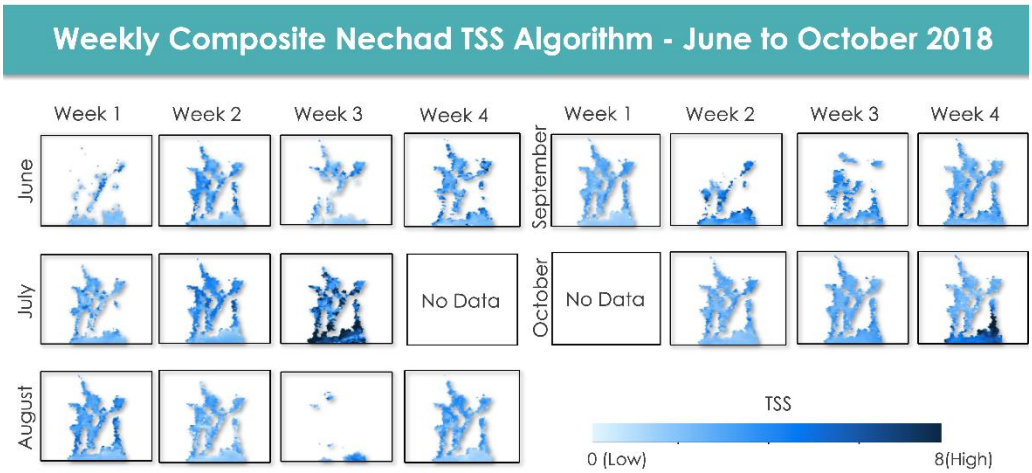

Figure E2. Weekly TSS values for 2018 visualized in SeaDAS with light blue representing low values and dark blue indicating high values.

Appendix F: *Weekly Composites for nFLH and TSS in the year 2022*

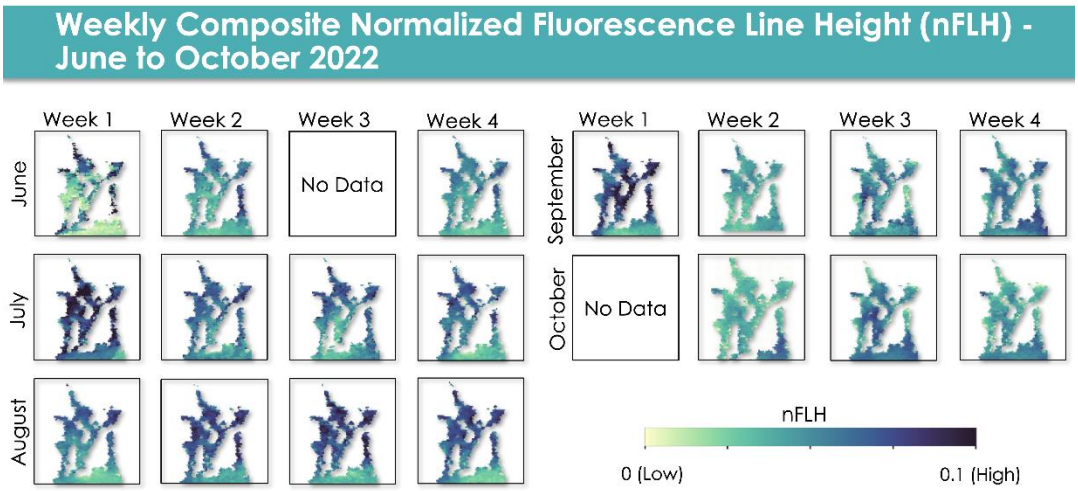

Figure F1. Weekly nFLH values for 2022 visualized in SeaDAS with yellow representing low values and dark blue indicating high values.

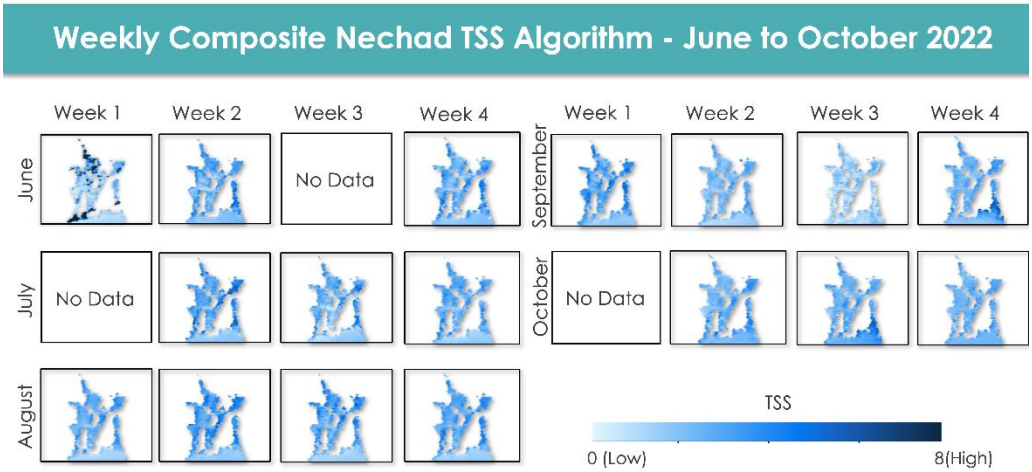

Figure F2. Weekly TSS values for 2022 visualized in SeaDAS with light blue representing low values and dark blue indicating high values.

Appendix G: *Map of RIDEM and EPA field measurement stations and data acquisition transect points*

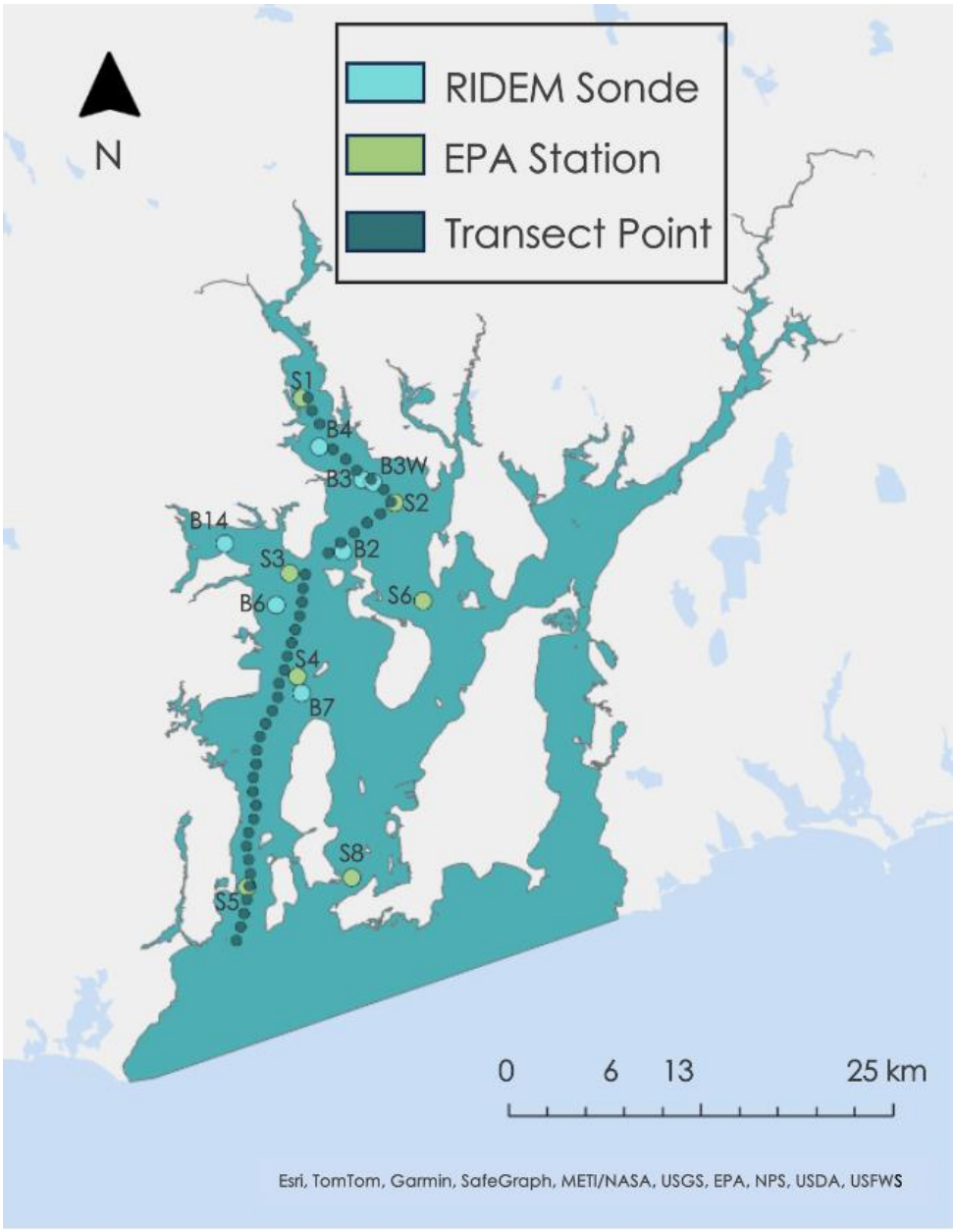

Figure G1. Map showing all the EPA and RIDEM field measurement stations and acquired satellite data transect points in the West Passage.